Penetration depth of single-, two-, and three-photon fluorescence microscopic imaging through human cortex structures: Monte Carlo simulation

Xiaoyuan Deng and Min Gu

Penetration depth is investigated in terms of the performance of transverse image resolution and signal level in human cortex under single-, two-, and three-photon fluorescence microscopy. Simulation results show that, in a double-layer human cortex structure consisting of gray and white matter media, the signal level is strongly affected by the existence of the white matter medium under three-photon excitation. Compared with three-photon excitation, two-photon excitation keeps a better signal level and sacrifices a slight degradation in image resolution. In a thick gray matter medium, a penetration depth of 1500 μm with a near-diffraction-limited resolution is obtainable under three-photon excitation. It is also demonstrated that the numerical aperture has a slight influence on image resolution and signal level under two- and three-photon excitation because of the nonlinear nature in the excitation process.

OCIS codes: 170.3660, 180.2520, 290.4020.

1. Introduction

Cortex is one of the most important parts of brain tissue and is involved in almost all functions of a brain such as perception, motor coordination, thought, emotion, intellect, memory, and so on. Brain cortex, especially gray matter, is a basic research object when brain functions and diseases are studied.

Imaging through brain cortex tissue can be achieved by many modalities, such as magnetic resonance imaging and positron emission tomography. However, optical microscopy offers the only way to achieve micrometer spatial resolution. In particular, fluorescence microscopy provides an effective way to investigate biological microstructures, to monitor biological activities, and to diagnose human disease.[1,2]

The authors are with the Centre for Micro-Photonics, School of Biophysical Sciences and Electrical Engineering, Swinburne University of Technology, P.O. Box 218, Hawthorn, Victoria 3122, Australia. The e-mail address for M. Gu is mgu@swin.edu.au.

Received 13 November 2002; revised manuscript received 21 January 2003.

0003-6935/03/163321-09$15.00/0

However, strong scattering by biological tissue in optical microscopy degrades image resolution and signal strength at a deep depth. In other words, scattering of light limits the imaging penetration depth of light. The emergence of multiphoton microscopy provides a tool to reduce scattering, enhances resolution, and thus leads to a deep penetration depth.[3–8] First, use of near-infrared light in multiphoton excitation reduces multiple scattering. Second, the simultaneous absorption of two or three photons results in a quadratic or cubic dependence of the fluorescence on the excitation intensity, which inherently provides a three-dimensional imaging ability and minimizes the photobleaching and photodamage outside of the focal region.[9]

Because of the advantages offered by multiphoton microscopy, a variety of experiments in rat brain, which aim at investigating neuron activities *in vivo*, have been undertaken with two-photon excitation[10–13], and the physical parameters that may influence the imaging penetration depth have been explored.[14] Brain cortex has a double-layer structure that is composed of gray and white matter, with gray matter lying on top. Gray matter contains neurons and provides the actual processing capacity, whereas white matter provides communications between different gray matter areas and between gray

matter and the rest of the tissue. Recently, scattering parameters in human brain cortex have been thoroughly investigated.[15] Therefore it is possible and meaningful to investigate the penetration depth through human brain cortex under multiphoton microscopy, which is important for the study of human brain disease in biopsy and autopsy.[16] The method presented in this paper is also applicable to the investigation of animal brain.

In this paper we present a detailed investigation into the penetration depth through brain cortex tissue in multiphoton fluorescence microscopy according to the double-layer Monte Carlo model developed recently.[17] The dependence of image resolution and signal level on the focal depth in a double-layer human cortex structure is revealed in Section 2. In Section 3, the effect of the numerical aperture of an imaging objective on these two parameters is investigated. The effect of the gray matter thickness on image resolution and signal level is studied in Section 4, and our conclusion is given in Section 5.

2. Transverse Resolution and Signal Level in a Double-Layer Human Cortex Structure under Single-, Two-, and Three-Photon Excitation

In this paper we use the concept of the effective point-spread function (EPSF)[18] to investigate transverse resolution (Γ) and signal level (η) along the focal depth under multiphoton fluorescence microscopy.[19] An EPSF through a turbid medium under a microscope can be defined by the distribution of photons in the focal region, which can propagate through a turbid medium, the aperture of a detection objective, and other optical apertures.[18]

Two steps are involved to derive an EPSF at a given focal plane in microscopic fluorescence imaging. First, an excited photon distribution $I_{ex}(r)$ (where r is the radial distance from the focus) is calculated with the Monte Carlo simulation, and the fluorescence photon distribution $p_n(r)$ is produced according to the weighting functions under one-photon ($1p$), two-photon ($2p$) and three-photon ($3p$) excitation, respectively[17]:

$$p_n(r) = \alpha_n I_{ex}^{\,n}(r)\,, \tag{1}$$

where $n = 1$, 2, and 3 corresponding to *1p*, *2p*, and *3p* excitation, respectively, and $\alpha_n = 1$ in this simulation. In the second step of the Monte Carlo simulation, fluorescence photons excited by Eq. (1) are monitored, and those fluorescence photons at r and reaching the detector lead to a photon distribution $h_n(r)$, which is called the EPSF.[18,19] The image intensity of a thin object with a fluorescence strength function $O(x, y)$ can thus be given by a convolution relation:

$$I_n(x, y) = \int\int_{-\infty}^{\infty} h_n\{[(x)^2 + (y)^2]^{1/2}\} \times O(x - x', y - y')\mathrm{d}x'\,\mathrm{d}y'. \tag{2}$$

However, the convolution relation does not hold in the axial direction because the EPSF does not have any axial space invariance because of the scattering process.[18] We can model only the in-focus imaging process using Eq. (2) and characterize the transverse resolution. Therefore transverse resolution Γ in this paper is characterized by the distance between the 90% and 10% intensity points of the image of a thin sharp fluorescent edge scanned in the x direction.[19,20]

Another parameter used in this paper to characterize the multiple-scattering process is signal level. The signal level η is defined as the number of fluorescence photons collected by the detector and normalized by the number of the fluorescence photons when no scattering exists (the thickness of the turbid medium is zero).[19] The normalization process eliminates the difference of the strength of the excitation process and thus allows an easy comparison of the relative decay rate of the fluorescence strength along the penetration depth. According to the definition of the signal level, the signal level in this paper represents the total contribution of fluorescence photons collected by the detector, which contain the fluorescence photons excited by ballistic photons, snake photons, and scattered photons as well. Although this definition of the signal level does not provide the direct information of resolution degradation, it is important to determine the resolution of the reconstructed image in image processing through turbid media.[21] The reason for this feature is that scattered photons also carry object information but in a complicated way. However, the convolution relation shown in Eq. (2) indicates that the object information can be extracted when we perform a deconvolution operation[21]; the more the object information is extracted, the higher the image resolution. As indicated in our previous paper,[21] achieving a stable deconvolution operation needs an input image with strong strength; otherwise the noise signal from sources other than a turbid sample can lead to pronounced artifacts in a deconvolved image.

A double-layer Monte Carlo simulation model adopted in this simulation is the same as that described elsewhere.[17] The Fresnel formulas are used to determine the internal reflection or transmittance of the photons on the boundaries and the interface. Illumination at 10^7 photons are used to ensure the accuracy of simulation results under *1p*, *2p*, and *3p* excitation, and the radial sampling resolution dr in the focus plane is 2 μm. The detector size in this paper is chosen to be large enough (infinite) to collect all the fluorescence photons incident on the objective lens and covered by the collection lens. The lenses for excitation and collection are identical.

According to a recent magnetic resonance imaging study,[22] the thickness of the gray matter layer is between 1000 and 4500 μm, and its average thickness is approximately 2500 μm. In this section, the thickness of the gray and white matter layers is assumed to be 1000 μm for a thorough investigation of the effect of the boundary between gray and white matter on image performance. This human cortex

Table 1. Absorption and Scattering Parameters of Human Cortex under *1p*, *2p*, and *3p* Excitation[a]

Human Cortex	Optical Parameters	Excitation Wavelength (nm) 400	800	1200
Gray matter	μa (1/mm)	0.25	0.05	0.017
	μs (1/mm)	12.5	7.8	5.53
	l (μm)	78.5	127.4	181
	g	0.85	0.87	0.91
White matter	μa (1/mm)	0.3	0.17	0.1
	μs (1/mm)	42	38	40.2
	l (μm)	23.6	26.2	25
	g	0.75	0.86	0.89

[a] μa, absorption coefficient; μs, scattering coefficient; l, scattering mean-free-path length; g, anisotropy value.

structure is named cortex1. The excitation wavelength for *1p*, *2p*, and *3p* excitation is assumed to be 400, 800, and 1200 nm, respectively, and the fluorescence wavelength is assumed to be 400 nm in all three cases. The optical parameters of gray and white matter in human cortex[15] that are adopted in this simulation are summarized in Table 1. It should be pointed out that the assumed fluorescence wavelength does not affect the conclusion of the investigation as the scattering parameters do not vary appreciably in the region near this wavelength.[15]

The *1p*, *2p*, and *3p* fluorescence EPSFs at the focal depths of 800, 1000, and 1200 μm in cortex1 are shown in Fig. 1 for an objective numerical aperture of 0.25. The focal depth f_d is defined to be the distance between the surface of the gray matter layer to the focal plane. It is clear that the focal depths of 800, 1000, and 1200 μm mean that the focus is within the gray matter layer, at the boundary, and within the white matter layer. It can be seen that, in all three cases, the EPSF under *1p* excitation is the broadest, and its difference from those under *2p* and *3p* excitation is significant, especially within the gray matter layer [Fig. 1(a)] and on the boundary [Fig. 1(b)]. The EPSFs under *2p* and *3p* excitation within the gray matter layer [Fig. 1(a)] are sharp and narrow, and the difference between them is almost undistinguishable [see the inset of Fig. 1(a)]. At the boundary, the difference of the EPSF between *2p* and *3p* excitation becomes slightly large [see the inset of Fig. 1(b)], showing the narrower EPSF under *3p* excitation. When the focus moves into the white matter layer, the EPSF under *1p*, *2p*, and *3p* excitation dramatically becomes broad [Fig. 1(c)]. The reason for this feature is that the white matter layer has a shorter scattering mean-free-path length (l) compared with that in the gray matter layer, which results in a stronger scattering effect and accordingly a dominant contribution of scattered photons in image formation.

Image resolution Γ and signal level η under *1p*, *2p*, and *3p* excitation along the entire cortex1 thickness are shown in Figs. 2(a) and 2(b), respectively. From Fig. 2 we can see that, only within a shallow depth in

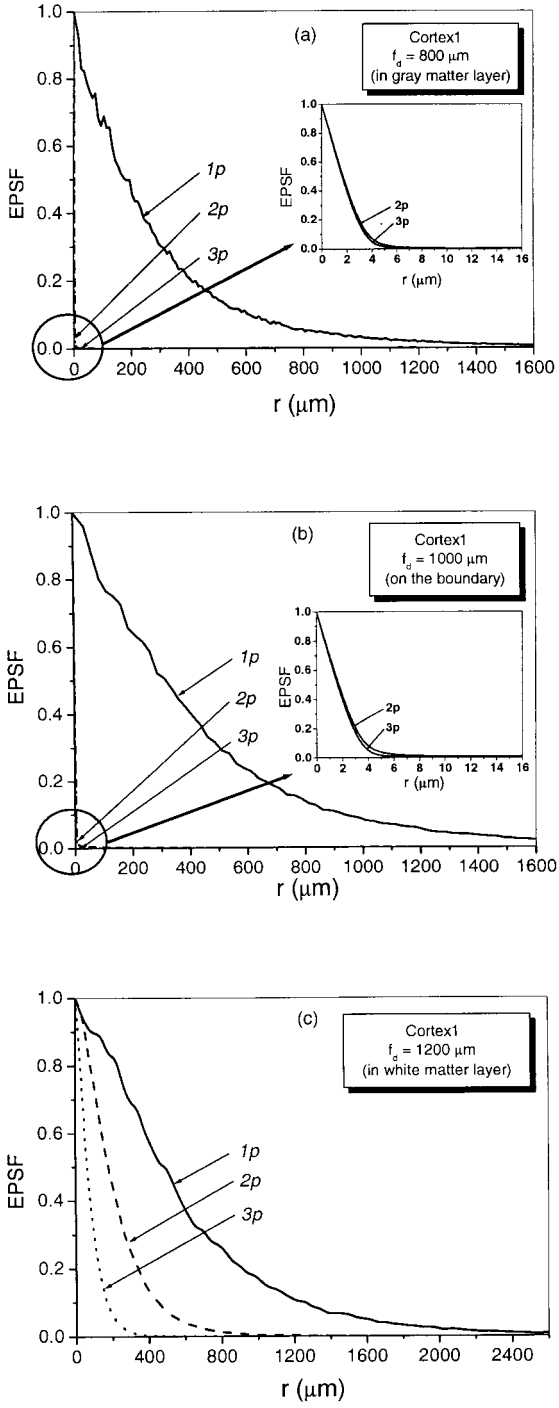

Fig. 1. Comparison of 1*p*, 2*p*, and 3*p* fluorescence EPSFs in cortex1 (numerical aperture is 0.25). (a) At the focal depth of 800 μm (within the gray matter layer); (b) at the focal depth of 1000 μm (on the boundary); (c) at the focal depth of 1200 μm (within the white matter layer).

gray matter ($f_d < 250$ μm), image resolution under *1p* excitation is better than 100 μm [Fig. 2(a)]. Image resolution under *2p* and *3p* excitation keeps the near-diffraction-limited value in the gray matter layer. The diffraction-limited resolution under *3p* excitation can be maintained almost up to the depth of 1000 μm (the whole range of the gray matter layer). How-

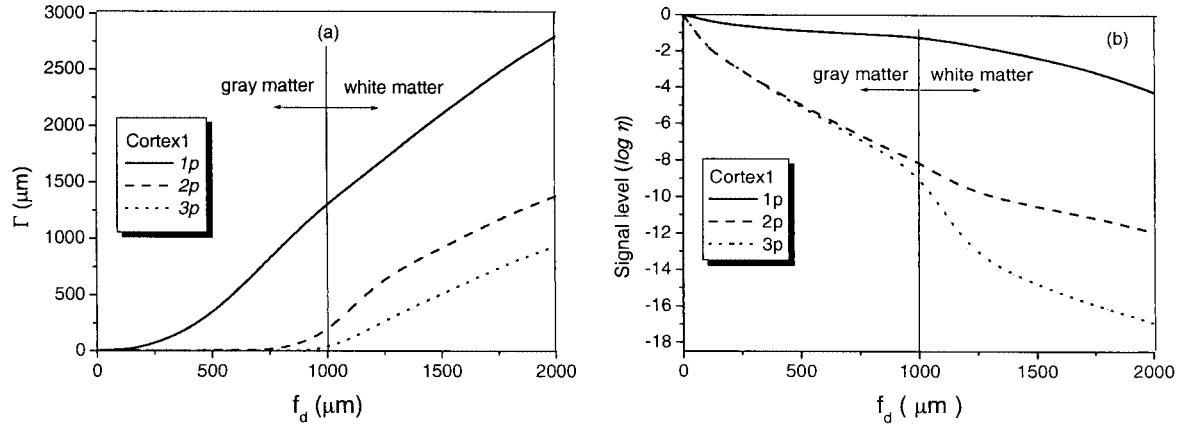

Fig. 2. (a) Transverse resolution Γ and (b) signal level as a function of the focal depth in cortex1 under *1p*, *2p*, and *3p* excitation (numerical aperture is 0.25).

ever, under *2p* excitation, the diffraction-limited resolution can be maintained only within a depth of 750 μm. This feature can be explained by the comparison of the scattering mean-free-path lengths shown in Table 1; the scattering mean-free-path length under *2p* and *3p* excitation within the gray matter layer is much longer than that under *1p* excitation. When the focus moves from the gray matter layer into the white matter layer, the resolution becomes degraded rapidly under *2p* and *3p* excitation because of the significant reduction of the scattering mean-free-path length from the gray matter layer to the white matter layer. The *3p* excitation results in the best image resolution in the white matter layer, showing that Γ in *3p* excitation is approximately 1.5 times better than that under *2p* excitation.

For signal level in coretx1 [Fig. 2(b)], we can see that the decrease in signal level under *1p* excitation is the slowest compared with *2p* and *3p* excitation at a given penetration depth. The signal level under *2p* and *3p* excitation has almost the same value until the depth of 1000 μm (on the boundary), which means that, within the whole gray matter region, *2p* and *3p* excitation makes no difference in terms of signal level. However, when the focal depth enters the white matter layer, the signal level under *3p* excitation drops more quickly than that under *2p* excitation. This property indicates that the larger reduction of the scattering mean-free-path length in the white matter layer under *3p* excitation has a more significant impact on the signal level than that under *2p* excitation.

3. Effect of the Objective Numerical Aperture on Transverse Resolution and Signal Level in Double-Layer Human Cortex

It should be pointed out that an image is formed in two steps in an image system. The first step is excitation and the second is collection. It should be also pointed out that both ballistic and scattered photons in the excitation process can result in fluorescence emission.[20] Only ballistic photons are confined to the focal region, and multiphoton excitation can help the confinement of ballistic photons, whereas scattered photons in the excitation process are distributed away from the focal region. In the collection process, these two types of photon behave differently. The contribution of scattered excitation photons is reduced under multiphoton excitation because of the nonlinear dependence of fluorescence emission. Both processes are affected by the value of the numerical aperture.[19] In this section, the effect of the objective numerical aperture on image formation under *1p*, *2p*, and *3p* excitation in the double-layer human cortex medium (cortex1) is investigated.

Figures 3(a) and 3(b) show the image resolution Γ and the signal level η in cortex1 under *1p* excitation for numerical apertures of 0.25 and 0.75. We can see that Γ is distinctly poorer as a higher numerical aperture objective is used. Under *1p* excitation, Beer's law indicates that scattered photons are dominant in image formation when the focal depth of the turbid medium is larger than a few scattering mean-free-path lengths. Even when there is only one scattering event, i.e., $f_d = l$, approximately 64% of the incident photons are scattered.[17] Therefore, according to Table 1, the contribution of scattered photons is dominant in the excitation and collection processes in the case of cortex1 when the focal depth is longer than 100 μm. Compared with the lower numerical aperture objective, the higher numerical aperture objective has a larger angle of convergence, and thus more scattered photons that deviate from the ballistic path can be collected by the objective. These scattering components do not satisfy the diffraction theory and make a significant contribution to image formation,[20] leading to the degradation of the image resolution. However, the larger the numerical aperture of an objective, the slower the dropping speed in the signal level [Fig. 3(b)].

Image resolution Γ and signal level η in cortex1 under *2p* excitation for different values of the objective numerical aperture are shown in Figs. 4(a) and 4(b), respectively. Unlike *1p* excitation, the objective numerical aperture under *2p* excitation produces

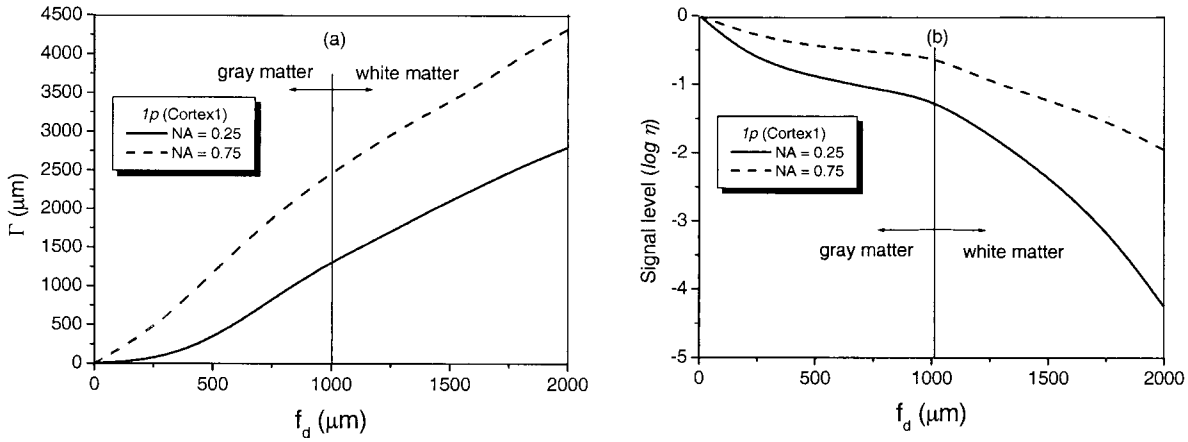

Fig. 3. (a) Transverse resolution Γ and (b) signal level for different values of the numerical aperture (NA) under *1p* excitation in cortex1.

a less pronounced influence on image resolution and signal level. Because of the quadratic dependence of the fluorescence on the excitation intensity under *2p* excitation, the contribution from the scattered photons to image formation is inherently weakened compared with that under *1p* excitation. Therefore the utilization of a high numerical aperture objective under *2p* excitation has a less pronounced influence on image performance.

Figures 5(a) and 5(b) are the illustration of transverse resolution and signal level under *3p* excitation in cortex1 for different values of the numerical aperture. Similar to *2p* excitation (Fig. 4), the cubic dependence of the fluorescence on the excitation intensity reduces the function of scattered photons on image formation, and thus a change in numerical aperture does not affect image formation significantly.

4. Effect of the Thickness of Gray Matter on Image Resolution and Signal Level

In Section 2, the gray matter layer with the thickness of 1000 μm, which corresponds to the thinnest thicknesses ranging from 1000 to 4500 μm reported by a magnetic resonance imaging study,[22] was investigated. To understand the effect of the thickness of gray matter on image formation, in this section the gray matter thickness of 2500 μm is selected. This sample is termed cortex2. For a comparison with the results in Section 3, image resolution and signal level only within the depth range from 0 to 2000 μm of cortex2 are plotted.

Figures 6(a) and 6(b) give image resolution and signal level in cortex2 under *1p*, *2p*, and *3p* excitation. The *1p* excitation leads to a slower drop in the signal level compared with that under *2p* and *3p* excitation, although it has a worse image resolution. In the whole region of the gray matter medium, *3p* excitation still has the best image resolution; the near-diffraction-limited image resolution can be maintained up to the depth of 1500 μm in this situation. When the focal depth is deeper than 1500 μm, Γ under *3p* excitation is approximately two times better than that under *2p* excitation. The reason for this feature can be explained as follows. Under *3p* excitation, a wavelength longer than that under *2p* excitation is adopted, and thus the scattering effect in the excitation process in gray matter is weaker in the

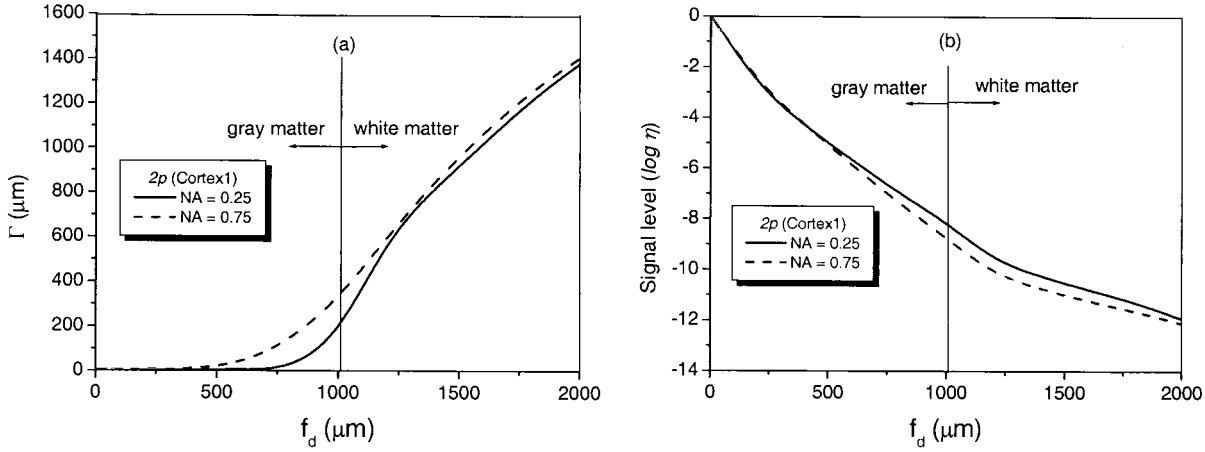

Fig. 4. (a) Transverse resolution Γ and (b) signal level for different values of the numerical aperture (NA) under *2p* excitation in cortex1.

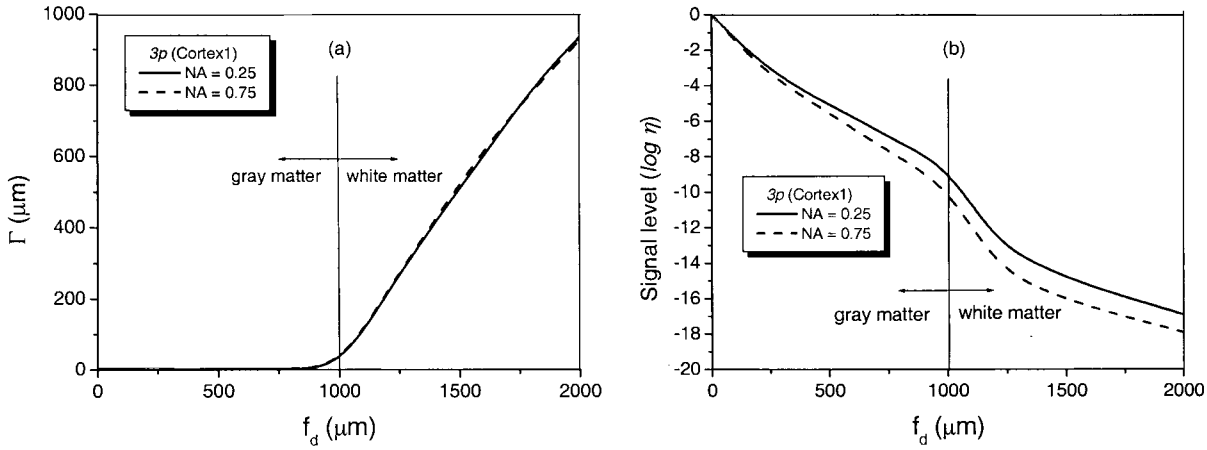

Fig. 5. (a) Transverse resolution Γ and (b) signal level for different values of the numerical aperture (NA) under *3p* excitation in cortex1.

former case, which can be confirmed from the *l* and *g* values given in Table 1. Furthermore, the higher-order nonlinear dependence of fluorescence on the excitation intensity under *3p* excitation reduces the influence of the scattered photons out of the focus plane, which finally results in a better transverse resolution. The signal level under *2p* and *3p* excitation exhibits a little difference up to the depth of 1000 μm. Beyond that point, *3p* excitation leads to a quicker drop in the signal level than that under *2p* excitation.

Comparing the image resolution and the signal level in cortex2 (see Fig. 6) with those in cortex1 (see Fig. 2), one can see that *3p* excitation is more sensitive to the white matter medium than *2p* excitation. Image resolution and signal level in cortex1 dramatically become worse when the second-layer medium is white matter (Fig. 2) rather than gray matter (Fig. 6). However, under *2p* excitation, both image resolution and signal level exhibit a slight change regardless of whether the second layer is white or gray matter.

For a comparison with cortex1, the effect of the numerical aperture objective on image resolution and signal level in cortex2 under *1p*, *2p*, and *3p* excitation is demonstrated in Figs. 7–9, respectively.

Under *1p* excitation, unlike the situation in cortex1 where the image resolution with a high numerical aperture objective is much poorer than that with a low numerical aperture objective [Fig. 3(a)], the difference in cortex2 is slight [Fig. 7(a)]. In cortex1 the second layer is white matter, whereas in cortex2 the second layer is the same as the first one, which is gray matter. Compared with gray matter, white matter has a shorter scattering mean-free-path length and a lower anisotropy value. Therefore the factor that results in the degradation of image resolution in cortex1 that is due to use of a high numerical aperture objective that may collect more photons strongly scattered from the white matter layer no longer exists in cortex2. This indicates that image quality under *1p* excitation by a high numerical aperture objective is more easily affected by the medium features compared with use of a low numerical aperture objective.

Under *2p* and *3p* excitation in cortex2 (Figs. 8 and 9), the effect of the numerical aperture is similar to that occurring in cortex1 (Figs. 4 and 5); the numer-

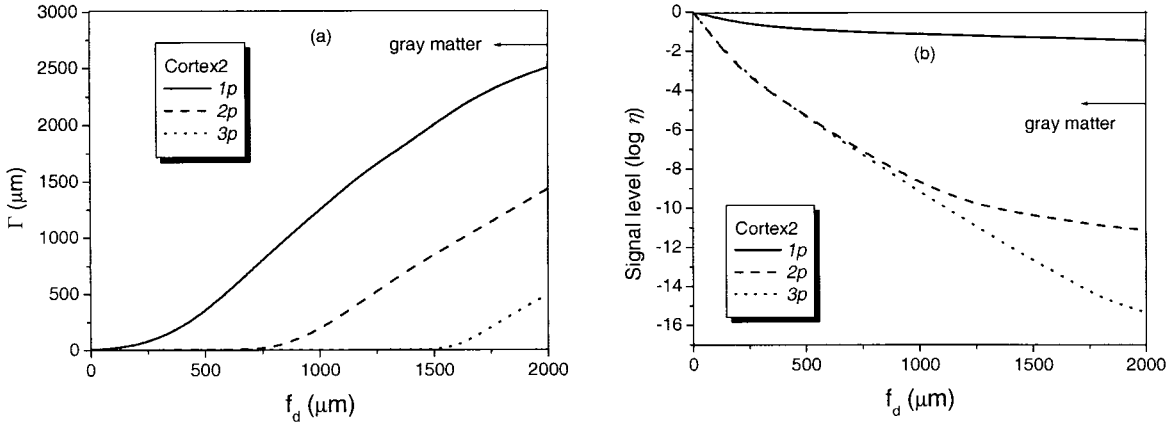

Fig. 6. (a) Transverse resolution Γ and (b) signal level as a function of focal depth under *1p*, *2p*, and *3p* excitation in cortex2 (numerical aperture is 0.25).

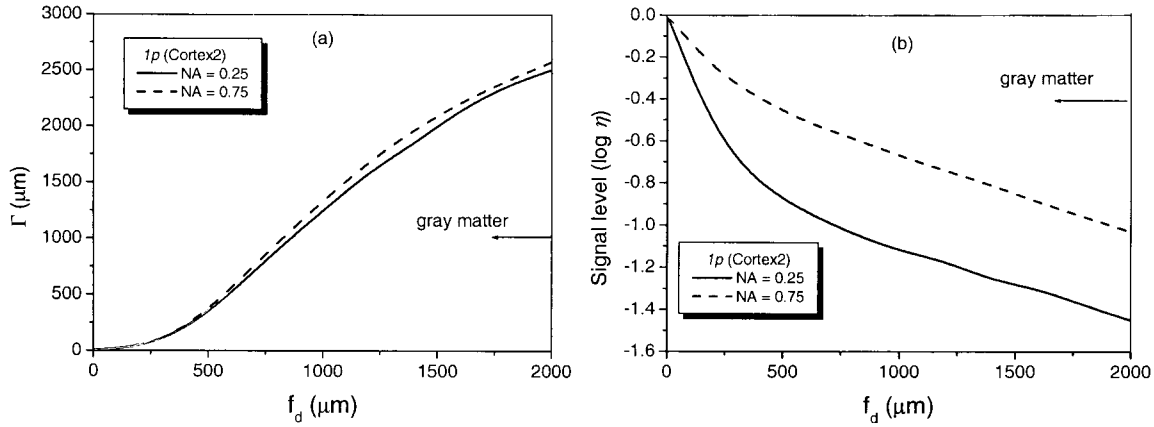

Fig. 7. (a) Transverse resolution Γ and (b) signal level for different values of the numerical aperture (NA) under *1p* excitation in cortex2.

ical aperture has a slight influence on image formation. However, we note that in cortex2 a cross point exists in the image resolution formed by the objective with the numerical apertures of 0.25 and 0.75 under *2p* excitation. This feature is caused by the competitive contributions from ballistic and scattered photons, as explained elsewhere.[19] Because of the joint contribution from ballistic and scattered photons, an optimized value of numerical aperture may occur for given scattering parameters of a turbid medium.

5. Discussion and Conclusion

In this paper, *1p*, *2p*, and *3p* fluorescence image resolution and signal level have been investigated as a function of the focal depth in human cortex, which consists of a gray matter layer and a white matter

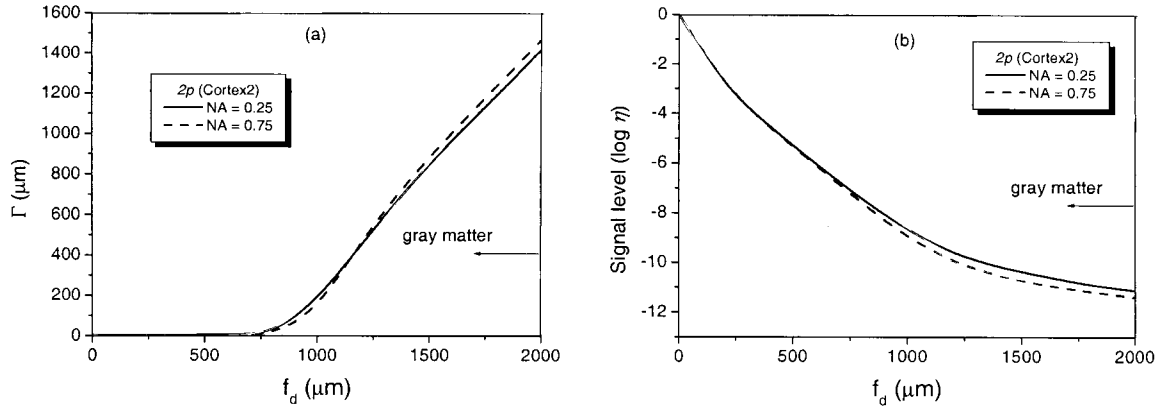

Fig. 8. (a) Transverse resolution Γ and (b) signal level for different values of the numerical aperture (NA) under *2p* excitation in cortex2.

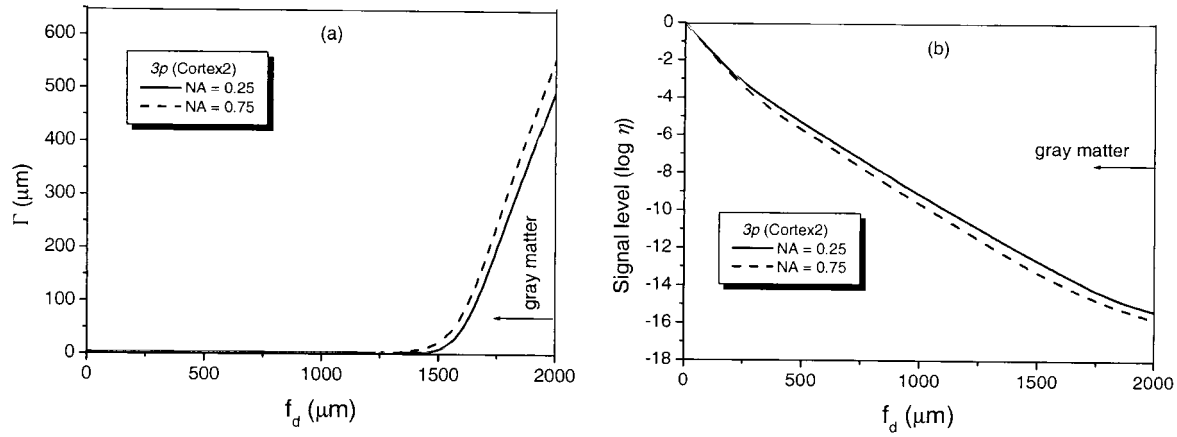

Fig. 9. (a) Transverse resolution Γ and (b) signal level for different values of the numerical aperture (NA) under *3p* excitation in cortex2.

layer. The effect of the gray matter thickness on image formation has also been explored. Furthermore, the function of the numerical aperture of an objective has been correspondingly discussed.

In the first sample (cortex1), although *3p* excitation has better image resolution than that under *2p* excitation, the signal level drops dramatically within the white matter layer. The *2p* excitation can maintain a relatively high signal level, but it sacrifices a slight degradation in image resolution. It should be pointed out that both ballistic and scattered photons result in fluorescence. When the contribution of ballistic photons is dominant, the fluorescence decay is exponential.[20,23] But this relation does not hold when scattered photons are dominant.[20,24] The diffraction-limited resolution can be kept up to the penetration depth of 700 μm under *2p* excitation within the gray matter layer, which is qualitatively comparable to the experimental penetration depth of 600 μm, although it may be limited by the available power in the rat brain.[25]

Imaging in the thick gray matter medium (cortex2) has shown *3p* excitation to be a better choice. The penetration depth of *3p* excitation with the diffraction-limited resolution can reach 1500 μm, and the dropping of the signal level is not as strong as that occurring in the white matter medium of cortex1. The *2p* excitation has a better signal level but its penetration depth is limited because the image resolution is approximately 2.5 times worse than that under *3p* excitation. Neurons in gray matter usually have diameters ranging from 4 to 100 μm. Therefore *3p* excitation can be used to image neurons up to a depth of 1000 μm with almost the same signal level as that under *2p* excitation if there is no power limit. A comparison of the results between cortex1 and cortex2 shows that the boundary between gray and white matter may lead to a further degradation of resolution because the scattered photons reflected by the boundary contribute to the image formation process.

For the effect of the objective numerical aperture, use of the lower numerical aperture objective is better for image resolution when scattered photons are dominant. However, the influence of the numerical aperture objective is not significant and can be neglected, especially under *2p* and *3p* excitation cases. Under *1p* excitation, the image resolution is strongly affected by use of a high numerical aperture objective in a medium with a small scattering mean-free-path length and a small anisotropy value.

The authors acknowledge the Australia Research Council for its support.

References

1. P. S. Andersson, S. Montan, and S. Svanberg, "Multispectral system for medical fluorescence imaging," IEEE J. Quantum Electron. **QE23,** 1798–1805 (1987).
2. W. A. Mohler and J. G. White, "Multiphoton laser scanning microscopy for four-dimensional analysis of caenorhabditis elegans embryonic development," Opt. Exp. **3,** 325–331 (1998); http://www.opticsexpress.org.
3. W. J. Denk, J. H. Strickler, and W. W. Webb, "Two-photon laser scanning fluorescence microscopy," Science **248,** 73–76 (1990).
4. M. Gu, "Resolution in three-photon fluorescence scanning microscopy," Opt. Lett. **21,** 988–990 (1996).
5. I. Gryczynski, H. Malak, and J. R. Lakowicz, "Three-photon induced fluorescence of 2,5-diphenyloxazole with a femetosecond Ti-sapphire laser," Chem. Phys. Lett. **245,** 30–35 (1995).
6. I. Gryczynski, H. Malak, and J. R. Lakowicz, "Three-photon excitation of a tryptophan derivative using a fs-Ti-sapphire laser," Biospectroscopy **2,** 9–15 (1996).
7. V. E. Centonze and J. G. White, "Multiphoton excitation provides optical sections from deeper within scattering specimens than confocal imaging," Biophys. J. **75,** 2015–2024 (1998).
8. W. Denk and K. Svoboda, "Photon upmanship: why multiphoton imaging is more than a gimmick," Neuron **18,** 351–357 (1997).
9. D. W. Piston, "Imaging living cells and tissues by two-photon excitation microscopy," Trends Cell Biol. **9,** 66–69 (1999).
10. S. Charpak, J. Mertz, E. Beaurepaire, L. Moreaux, and K. Delaney, "In vivo two-photon imaging of odor-evoked calcium signals in dentrites of rat mitral cells," Proc. Natl. Acad. Sci. USA **98,** 1230–1234 (2001).
11. K. Svoboda, W. Denk, D. Kleinfeld, and D. W. Tank, "In vivo dentritic calcium dynamics in neocortical pyramid neurons," Nature (London) **385,** 161–165 (1997).
12. F. Helmchen, K. Svoboda, W. Denk, and D. W. Tank, "In vivo denfritic calcium dynamics in deep-layer cortical pyramidal neurons," Nature Neurosci. **2,** 989–996 (1999).
13. K. Svoboda, F. Helmchen, W. Denk, and D. W. Tank, "Spread of dendritic excitation in layer 2/3 pyramidal neurons in rat barrel cortex in vivo," Nature Neuronsci. **2,** 65–73 (1999).
14. M. Oheim, E. Beaurepaire, E. Chaigneau, J. Mertz, and S. Charpak, "Two-photon microscopy in brain tissue: parameters influencing the imaging depth," J. Neurosci. Methods **111,** 29–37 (2001).
15. H. J. Schwarzmaier, A. Yaroslavsky, I. Yaroslavsky, T. Goldbach, T. Kahn, F. Ulrich, P. C. Schulze, and R. Schober, "Optical properties of native and coagulated human brain structures," in *Lasers in Surgery: Advanced Characterization, Therapeutics, and System VII,* R. Anderson, K. E. Bartels, L. S. Bass, K. W. Gregory, D. M. Harris, H. Lui, R. S. Malek, G. T. Mueller, M. M. Pankratov, A. P. Perlmutter, H. Reidenback, L. P. Tate, and G. W. Watson, eds., Proc. SPIE **2970,** 492–499 (1997).
16. P. Lenz, "Fluorescence measurement in thick tissue layers by linear or nonlinear long-wavelength excitation," Appl. Opt. **38,** 3662–3669 (1999).
17. X. Y. Deng, X. S. Gan, and M. Gu, "Multiphoton fluorescence microscopic imaging through double-layer turbid tissue media," J. Appl. Phys. **91,** 4659–4665 (2002).
18. X. S. Gan and M. Gu, "Effective point-spread function for fast image modeling and processing in microscopic imaging through turbid media," Opt. Lett. **24,** 741–743 (1999).
19. X. S. Gan and M. Gu, "Fluorescence microscope imaging through tissue-like turbid media," J. Appl. Phys. **87,** 3214–3221 (2000).
20. M. Gu, X. S. Gan, A. Kisteman, and M. Xu, "Comparison of penetration depth between single-photon excitation and two-photon excitation in imaging through turbid tissue media," Appl. Phys. Lett. **77,** 1551–1553 (2000).
21. X. S. Gan and M. Gu, "Microscopic image reconstruction through tissue-like turbid media," Opt. Commun. **207,** 149–154 (2002).
22. B. Fischl and A. M. Dale, "Measuring the thickness of the human cerebral cortex from magnetic resonance images," Proc. Natl. Acad. Sci. USA **97,** 11044–11049 (2000).

23. A. K. Dunn, V. P. Wallace, M. Coleno, M. W. Berns, and B. J. Tromberg, "Influence of optical properties on two-photon fluorescence imaging in turbid samples," App. Opt. **39,** 1194–1201 (2000).
24. V. Daria, C. M. Blanca, O. Nakamura, S. Kawata, and C. Saloma, "Image contrast enhancement for two-photon fluorescence microscopy in a turbid medium," Appl. Opt. **37,** 7960–7967 (1998).
25. D. Kleinfeld, P. P. Mitra, F. Helmchen, and W. Denk, "Fluctuation and stimulus-induced changes in blood flow observed in individual capillaries in layer 2 through 4 of rat neocortex," Proc. Natl. Acad. Sci. USA **95,** 15741–15746 (1998).